

Kinematics of the Shoulder Joint in Tennis Players

Lädemann A,^{1,2} Chagué S,³ Kolo FC,⁴ Charbonnier C³

¹ *Division of Orthopaedics and Trauma Surgery, La Tour Hospital, Geneva, Switzerland*

² *Faculty of Medicine, University of Geneva, Geneva, Switzerland*

³ *Artanim Foundation, Medical Research Department, Geneva, Switzerland*

⁴ *Rive Droite Radiology Center, Geneva, Switzerland*

1 **ABSTRACT**

2 Background: Shoulder pain and injury are common in tennis players. The precise
3 causes for such pain remain unclear. Impingement at critical tennis positions and
4 glenohumeral instability have never been dynamically evaluated in-vivo. The purpose
5 of this study was to evaluate the different types of impingement and stability during
6 tennis movements.

7 Methods: Type and frequency of impingement as well as percentage of subluxation
8 were evaluated in 10 tennis players through a novel dedicated patient-specific
9 measurement technique based on optical motion capture and Magnetic Resonance
10 Imaging (MRI).

11 Results: All volunteers, nine male and one female, had a clinically functional rotator
12 cuff. MRI revealed 11 rotator cuff lesions in six subjects and six labral lesions in five
13 subjects. Lateral subacromial, anterior subacromial, internal anterosuperior, and
14 internal posterosuperior impingements were observed in four, three, two and seven
15 subjects, respectively. No instability could be demonstrated in this population.

16 Conclusion: Tennis players presented frequent radiographic signs of structural
17 lesions that could mainly be related to posterosuperior impingements due to
18 repetitive abnormal motion contacts. This is the first study demonstrating that a
19 dynamic and precise motion analysis of the entire kinematic chain of the shoulder is
20 possible through a non-invasive method of investigation. This premier kinematic
21 observation offers novel insights into the analysis of shoulder impingement and
22 instability that could, with future studies, be generalized to other shoulder pathologies
23 and sports. This original method may open new horizons leading to improvement in
24 impingement comprehension.

25 Keywords: Shoulder kinematics modeling; Biomechanics, Tennis players; Overhead
26 athletes; Impingement; Magnetic resonance imaging.

27 INTRODUCTION

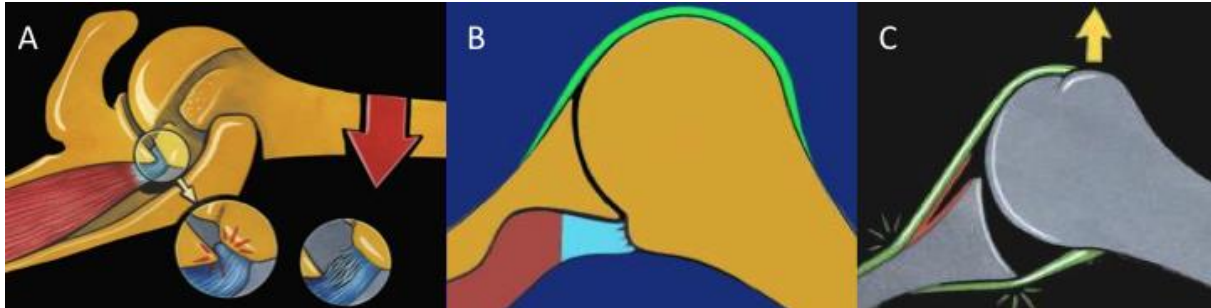
28 Shoulder pain and injury are common in tennis players, with a prevalence of 50% for
29 certain categories of age.¹ A majority of shoulder pain is caused by impingement and
30 instability due to repetitive lifting and overhead arm movements. Two types of
31 impingement have been described: external and internal. External types include
32 subacromial impingement of the rotator cuff between the anterior acromion² or lateral
33 acromion³ and the superior humeral head that could occur with serves and overhead
34 shots. Another type of external impingement is the less common subcoracoid
35 impingement⁴ of the subscapularis or biceps tendon. It results from contact between
36 the coracoid process against the lesser tuberosity of the humeral head and is more
37 likely to occur at the backhand preparation phase and the late follow-through phase
38 of the forehand. Internal impingement consists of (1) posterosuperior impingement⁵
39 of the supraspinatus and infraspinatus tendons between the greater tuberosity of the
40 humeral head and the posterosuperior aspect of the glenoid when the arm is in
41 extreme abduction, extension and external rotation during the late cocking stage of
42 the serve; and (2) anterosuperior impingement⁶ of the deep surface of the
43 subscapularis tendon and the reflection pulley on the anterosuperior glenoid rim that
44 could also occur at the backhand preparation phase and the late follow-through
45 phase of forehand.

46 The precise causes for these impingements remain unclear, but it is believed that
47 repetitive contact (Figure 1A and 1B), glenohumeral instability (Figure 1C), scapular
48 orientation, rotator cuff dysfunction, and posteroinferior capsular contracture with
49 resultant glenohumeral internal rotation deficit (GIRD) may play a role in the
50 development of symptomatic impingement.^{5,7,8} Measuring the dynamic in-vivo
51 shoulder kinematics seems crucial to better understand these pathologies and to

52 propose an adequate treatment. Indeed, a patient with an internal impingement will
53 be treated differently if the etiology is a posteroinferior capsular contracture with
54 resultant GIRD (that generally responds positively to a compliant posteroinferior
55 capsular stretching program or to an arthroscopic selective posteroinferior
56 capsulotomy and concomitant partial articular sided tendon avulsion (SLAP) lesion
57 repair⁹) or a repetitive contact of the undersurface of the rotator cuff on the
58 posterosuperior glenoid labrum (that can respond to debridement, glenoidplasty or
59 derotational humeral osteotomy).¹⁰⁻¹² However, such kinematic measurements
60 remain a challenging problem due to the complicated anatomy and large range of
61 motion of the shoulder. To our knowledge, impingements at critical tennis positions
62 and glenohumeral stability have never been dynamically evaluated. Unfortunately,
63 the motion of the shoulder cannot be explored with standard Magnetic Resonance
64 Imaging (MRI) or Computed Tomography (CT) because they are limited by space
65 and the velocity of the movement and might therefore miss dynamic motion.
66 Fluoroscopy-based measurements provide sufficient accuracy for dynamic shoulder
67 analysis,¹³ but they use ionizing radiation. Motion capture systems using skin-
68 mounted markers provide a non-invasive method to determine shoulder kinematics
69 during dynamic movements.¹⁴ However, none of the current motion capture
70 techniques have reported translation values at the glenohumeral joint. One reason
71 that might explain this void is that current techniques have either concentrated their
72 efforts on the analysis of a single shoulder bone (e.g., scapula) or focused on the
73 description of humeral motion relative to the thorax rather than to its proximal bone.

74 The purpose of the study was thus: (1) to develop a dedicated patient-specific
75 measurement technique based on optical motion capture and MRI to accurately
76 determine glenohumeral kinematics (rotations and translations) taking into account

77 the whole kinematic chain of the shoulder complex from the thorax to the humerus
78 through the clavicle and scapula, (2) to evaluate impingement, stability, and other
79 motion-related disorders during dynamic movements in high-level tennis players.



80

81 **Figure 1:** (A) Gilles Walch's theory: the deep layer of the posterosuperior rotator cuff
82 impinged with the posterior labrum and glenoid. (B) Christopher Jobe's theory: the
83 impingement is mainly due to hyperextension of the humerus relative to the scapula. (C)
84 Frank Jobe's theory: lesions in throwing athletes are related to subtle anterior instability.

85

86 **METHODS**

87 Ten volunteers who were intermediate or ex-professional tennis players were
88 recruited for this study. Ethical approval was gained from the local Institutional
89 Review Board, and all participants gave their written informed consent prior to taking
90 part in the study. Exclusion criteria were reported previous shoulder injuries, shoulder
91 surgery or contraindications for MRI.

92 The outcomes of interest were the prevalence of internal and external
93 impingement and glenohumeral instability in this particular population. Furthermore,
94 the prevalence of other radiographic pathologies was evaluated in relation to the
95 main outcomes of interest. The following baseline characteristics were assessed:
96 age, sex, body mass index, shoulder side, and limb dominance.

97 Rotator cuff examination included the belly-press, bear hug, Jobe tests, and
98 external rotation strength against resistance. Constant score,¹⁵ American Shoulder and
99 Elbow Surgeons (ASES) score,¹⁶ a single assessment numeric evaluation (SANE)

100 score,¹⁷ and a visual analog scale (VAS) pain score graded from 0 points (no pain) to
101 10 points (maximal pain) were recorded.

102 All volunteers underwent an MR shoulder arthrography. The MRI examinations
103 were conducted after a fluoroscopically guided arthrography with a contrast agent
104 and with an anterior approach. MRI was performed with a 1.5 T HDxT system
105 (General Electric Healthcare, Milwaukee WI, USA). A dedicated shoulder surface coil
106 was used. A sagittal T1 weighted fast spin echo sequence, a coronal and sagittal T2
107 weighted fast spin echo sequence with fat saturation, a coronal and axial T1
108 weighted fast spin echo sequence with fat saturation, and three 3D fast gradient echo
109 (Cosmic® and Lava®) sequences were achieved. Table 1 details the imaging
110 parameters of each MRI sequence.

111 MR arthrograms were assessed by a musculoskeletal radiologist for shoulder
112 pathology including rotator cuff, labral or ligament (HAGL) lesion and bony changes.

113 Based on the 3D MR images, patient-specific 3D models of the shoulder bones
114 (humerus, scapula, clavicle and sternum) were reconstructed for each volunteer
115 using ITK-SNAP software (Penn Image Computing and Science Laboratory,
116 Philadelphia, PA).

117 Kinematic data was recorded using a Vicon MX T-Series motion capture system
118 (Vicon, Oxford Metrics, UK) consisting of 24 cameras (24 × T40S) sampling at 240
119 Hz. The volunteers were equipped with spherical retroreflective markers placed
120 directly onto the skin using double-sided adhesive tape (Figure 2). Four markers (Ø
121 14 mm) were attached to the thorax (sternal notch, xyphoid process, C7 and T8
122 vertebra). Four markers (Ø 6.5 mm) were placed on the clavicle. Four markers (Ø 14
123 mm) were fixed on the upper arm, two placed on anatomical landmarks (lateral and
124 medial epicondyles) and two as far as possible from the deltoid. For the scapula, one

125 marker (\varnothing 14 mm) was fixed on the acromion. In addition, the scapula was covered
126 with 56 markers (\varnothing 6.5 mm) to form a 7x8 regular grid. Finally, additional markers
127 were distributed over the body (non-dominant arm and legs).



128

129

Figure 2: Markers placement.

130 After appropriate warm-up, participants were asked to perform the following tennis
131 movements: forehand, backhand, flat and kick serves. They were also instructed to
132 perform three motor tasks: internal-external rotation of the arm with 90° abduction
133 and the elbow flexed 90°, flexion of the arm from neutral to maximum flexion, and
134 empty-can abduction from neutral to maximum abduction in the scapular plane.
135 Three trials of each motion were recorded. The same investigators attached all
136 markers and performed all measurements.

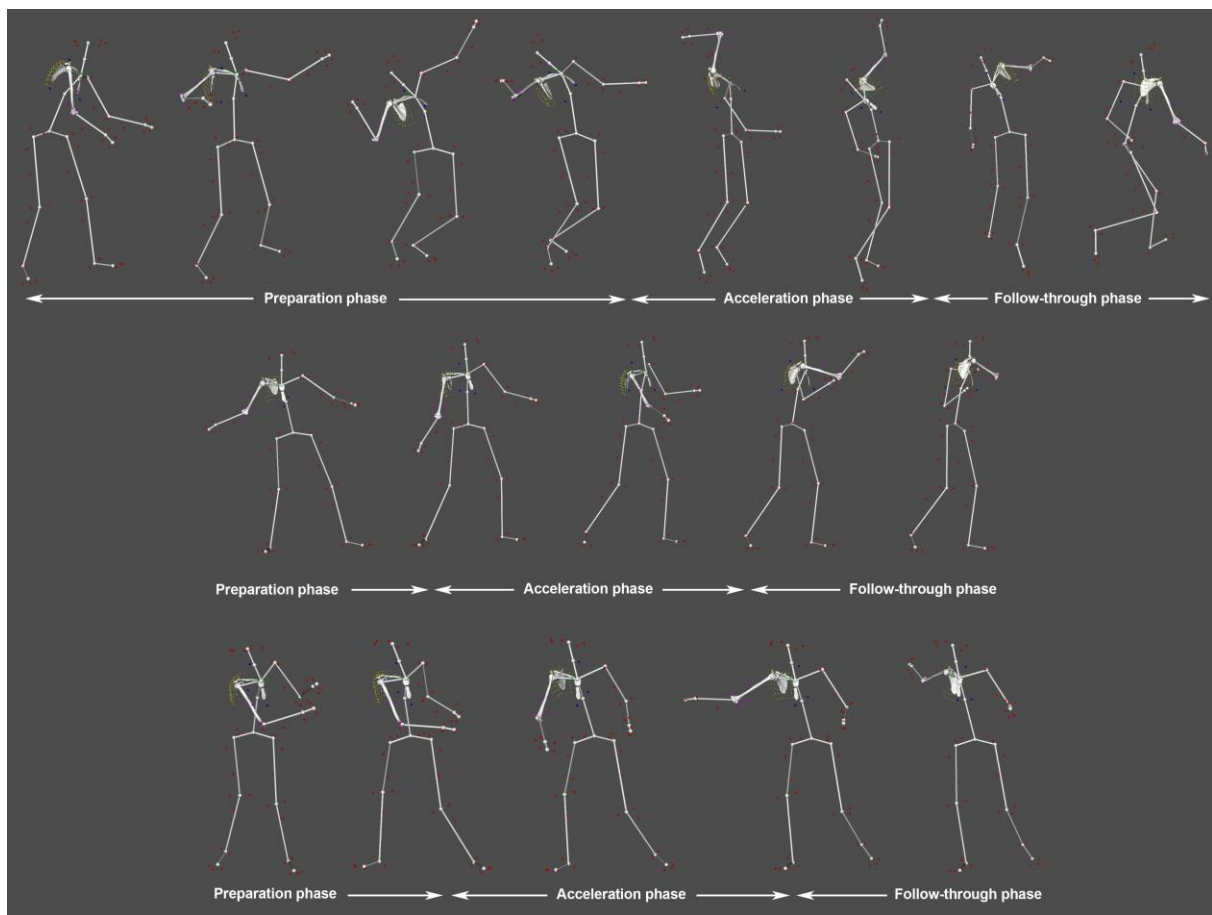
137 Shoulder kinematics were computed with custom-made software using the
138 recorded markers' trajectories. The major drawback with optical motion capture
139 systems is the soft tissue deformation due to muscle contractions and skin sliding,
140 causing marker movements with respect to the underlying bones. In the upper
141 extremity, the scapula is particularly affected. To solve this issue, it was
142 demonstrated that the use of global optimization could help reduce soft tissue
143 artifacts (STA) errors globally.¹⁸ Therefore, we developed a patient-specific kinematic

144 chain model of the shoulder complex (including the thorax, clavicle, scapula and
145 humerus) using the subject's 3D bony models¹⁹. The shoulder joints were each
146 modeled as a ball-and-socket joint (3 degrees of freedom) with loose constraints on
147 joint translations. The optimal pose of the kinematic chain was then obtained using a
148 global optimization algorithm. To verify its accuracy, kinematic data was collected
149 simultaneously from an X-ray fluoroscopy unit (MultiDiagnost Eleva, Philips Medical
150 Systems, The Netherlands) and the motion capture system during clinical motion
151 patterns (flexion, abduction and internal-external rotation of the arm) in a validation
152 test. Glenohumeral kinematics were derived from the marker position data and
153 compared with the one obtained with the fluoroscopy gold-standard.^{13,19} The
154 accuracy of the model for glenohumeral orientation was within 4° for each anatomical
155 plane and between 1.9 and 3.3 mm in average for glenohumeral translation.
156 Moreover, the results showed that the translation patterns computed with the model
157 were in good agreement with previous research.²⁰

158 Finally, the computed motions were applied to the tennis player's shoulder 3D
159 models reconstructed from their MRI data. Figure 3 shows examples of computed
160 tennis positions. A ball and stick representation of the overall skeleton was also
161 added to improve the analysis and visualization of the motion. The method is
162 summarized in video 1.

163 To permit motion description of the shoulder kinematic chain, local coordinate
164 systems (Figure 4) were established based on the definitions suggested by the
165 International Society of Biomechanics²¹ to represent the thorax, clavicle, scapula and
166 humerus segments using anatomical landmarks identified on the subject's bony 3D
167 models. The glenohumeral joint center was calculated based on a sphere fitting

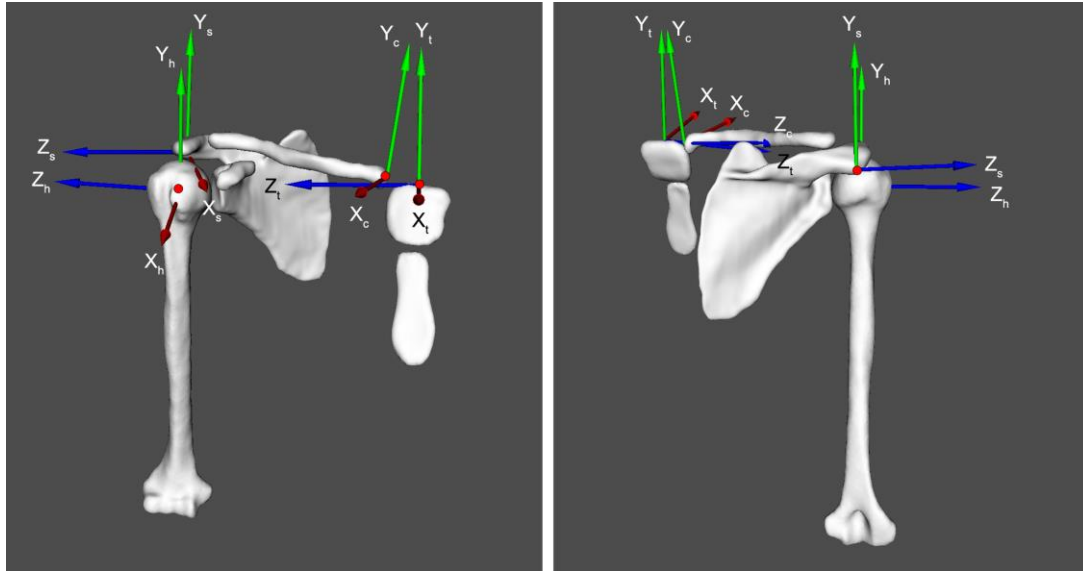
168 method²² that fits the optimal sphere to the humeral head using the points of the 3D
169 humeral model.



170
171 **Figure 3:** Computed tennis positions (here the right shoulder) according to the three main
172 phases, showing the markers setup (small colored spheres) and the virtual skeleton. Top:
173 serve shot. Position 4, 7 and 8 are commonly known as the cocking, deceleration and finish
174 stages, respectively. Middle: forehand shot. Bottom: backhand shot.

175 Glenohumeral range of motion (ROM) was quantified for flexion, abduction and
176 internal-external rotation movements. This was obtained by calculating the relative
177 orientation between the scapula and humerus coordinate systems at each point of
178 movement and then expressed in clinically recognizable terms (flex/ext, abd/add and
179 IR/ER) by decomposing the relative orientation into three successive rotations. It is
180 important to note that these computations were performed independently from the
181 major anatomical planes (i.e., sagittal, transverse, frontal planes). To facilitate clinical

182 comprehension and comparison, motion of the humerus with respect to the thorax
183 was also calculated. This was achieved with the same method but using the thorax
184 and humerus coordinate systems.



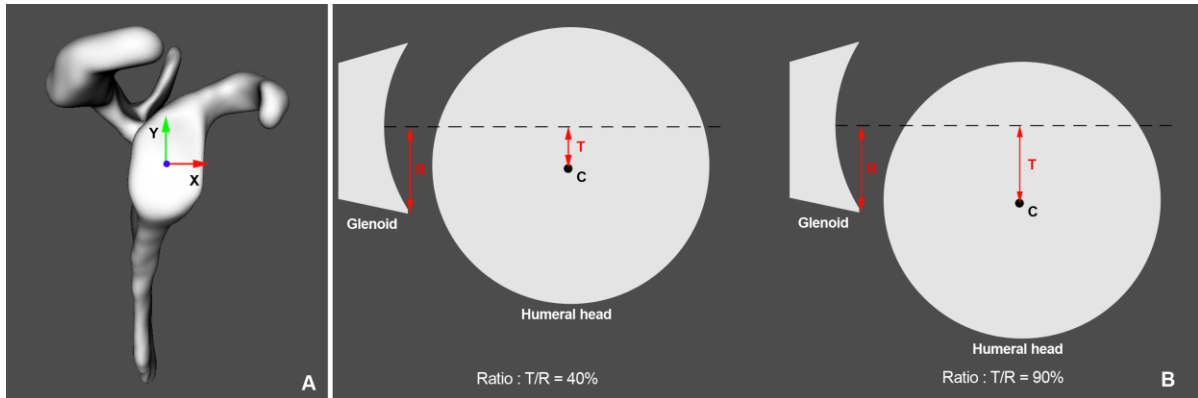
185

186 **Figure 4:** Bone coordinate systems for the thorax ($X_t Y_t Z_t$), clavicle ($X_c Y_c Z_c$), scapula ($X_s Y_s$
187 Z_s) and humerus ($X_h Y_h Z_h$).

188 Glenohumeral stability was assessed during flexion and abduction movements
189 and during flat and kick serves at the late cocking, deceleration and finish stages.
190 Glenohumeral translation was defined as anterior-posterior and superior-inferior
191 motion of the humeral head center relative to the glenoid coordinate system. This
192 coordinate system was determined by an anterior-posterior X-axis and a superior-
193 inferior Y-axis with origin placed at the intersection of the anteroposterior aspects and
194 superoinferior aspects of the glenoid rim (Figure 5A). Subluxation was defined as the
195 ratio (in %) between the translation of the humeral head center and the radius of
196 width (anteroposterior subluxation) or height (superoinferior subluxation) of the
197 glenoid surface (Figure 5B). Instability was defined as subluxation >50%.

198 Impingement was evaluated at critical tennis positions. While visualizing the tennis
199 player's shoulder joint in motion, minimum humero-acromial, humero-coracoid and

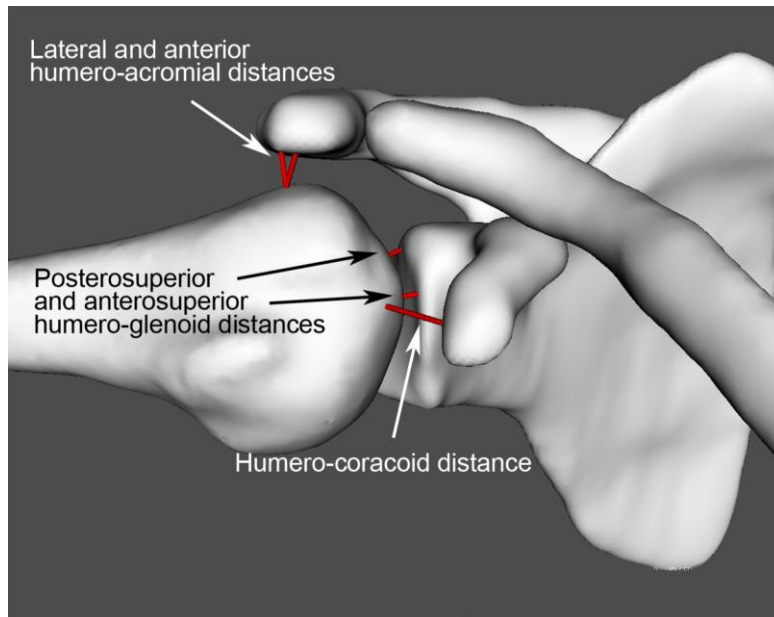
200 humero-glenoid distances that are typically used for the diagnosis of impingement
201 were measured (Figure 6). The distances were calculated in 3D based on position of
202 the simulated bone's model and were reported in millimeters.



203
204 **Figure 5:** (A) Definition of the glenoid coordinate system used in this study. (B) Schematic
205 representation of glenohumeral subluxation (C = center of the humeral head; R = radius of
206 the width or height of the glenoid surface; T = translation of the humeral head center). Left:
207 the ratio is 40%, there is no instability. Right: the ratio is >50%, instability is noted.

208 Given the thickness of the potential impinged tissues, impingement was
209 considered when the computed distance was <6 mm for the humero-acromial
210 distance and <5 mm for the other distances, as suggested in previous studies.²³⁻²⁵

211 For the three trials of flexion, abduction and internal-external rotation movements,
212 we computed the mean values and the standard deviations (SD) of the ROM at the
213 maximal range of motion. For all critical tennis positions, we calculated the frequency
214 of impingement and the mean and SD of the minimum humero-acromial, humero-
215 coracoid and humero-glenoid distances. We also computed the percentage of
216 subluxation at the different stages of serve. Finally, we analyzed glenohumeral
217 translations at the different elevation angles during flexion and abduction
218 movements.



219

220 **Figure 6:** Visualization of the humero-acromial, humero-coracoid and humero-glenoid
 221 distances during motion. The red lines represent the minimum distances.

222

223 **RESULTS**

224 The ten volunteers, nine male and one female, had all been playing tennis for more
 225 than 17 years. The mean \pm SD age, weight, height and body mass index of the
 226 subjects were 39.7 ± 8.9 years, 180.2 ± 7.1 cm, 76.7 ± 8.62 kg, and 23.5 ± 1.9 kg/m²,
 227 respectively. Nine volunteers were right-handed.

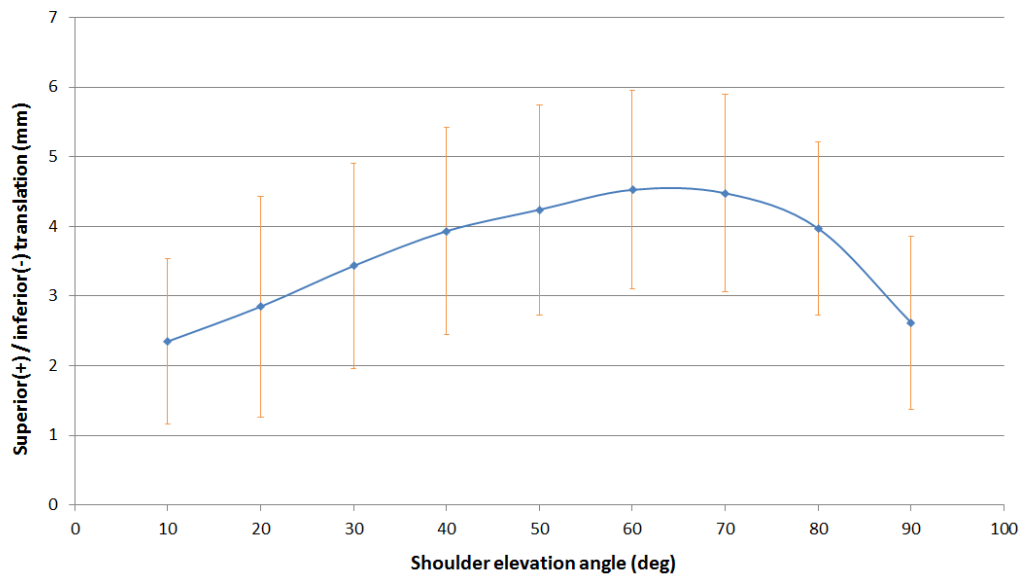
228 None of the tennis players displayed sudden loss of serving ability during the late
 229 cocking stage (so-called “dead arm”). All subjects had a competent rotator cuff. The
 230 mean Constant, ASES, SANE and VAS pain scores were 99.2 ± 1.4 points (range,
 231 96 to 100 points), 99.5 ± 1.6 points (range, 95 to 100 points), 95.0 ± 7.5 points
 232 (range, 80 to 100 points) and 0.6 ± 1.3 points (range, 0 to 4 points), respectively.
 233 Only 2 of the 10 subjects reported shoulder pain at the time of the examination. Nine
 234 had a history of shoulder pain during their career. Shoulder ROM determined by
 235 motion capture during clinical motor tasks are shown in Table 2. None of the tennis
 236 players had 180° ROM in internal-external rotation.

237 MR images revealed 11 rotator cuff lesions in six subjects (three interstitial tears of
238 the supraspinatus and PASTA tears in three supraspinatus, three infraspinatus and
239 two subscapularis tendons), and 6 labral lesions in five subjects (two inferior, two
240 posterior and two posterosuperior). There was no radiographic evidence of Bennett
241 lesions, thrower's exostosis, intraosseous cysts or Bankart lesions.

242 The type and prevalence of impingement and the bony distances are summarized
243 in Table 3. No subcoracoid impingement was detected during the late follow-through
244 phase of forehand or the backhand preparation phase, but anterosuperior
245 impingement was observed in two subjects during forehand (29% of the cases).
246 Anterior and lateral subacromial impingement occurred during the late cocking stage
247 of serve in three and four subjects, respectively. Posterosuperior impingement during
248 the late cocking stage of serve was the most frequent (seven subjects, 75% of the
249 cases). In this position, glenohumeral translation was anterior (flat serve, mean: 34%;
250 kick serve, mean: 34%) and superior (flat serve, mean: 12%; kick serve, mean: 13%),
251 as shown in Table 4. During the deceleration stage of serve, anterior and superior
252 translation varied from 8% to 57% and from 5% to 34%, respectively. During the
253 finish stage of serve, anterior translation was slightly more intense (flat serve, mean:
254 46%; kick serve, mean: 42%), while superior translation remained low (flat serve,
255 mean: 3%; kick serve, mean: 0%). There was no static posterosuperior shift of
256 glenohumeral contact point.

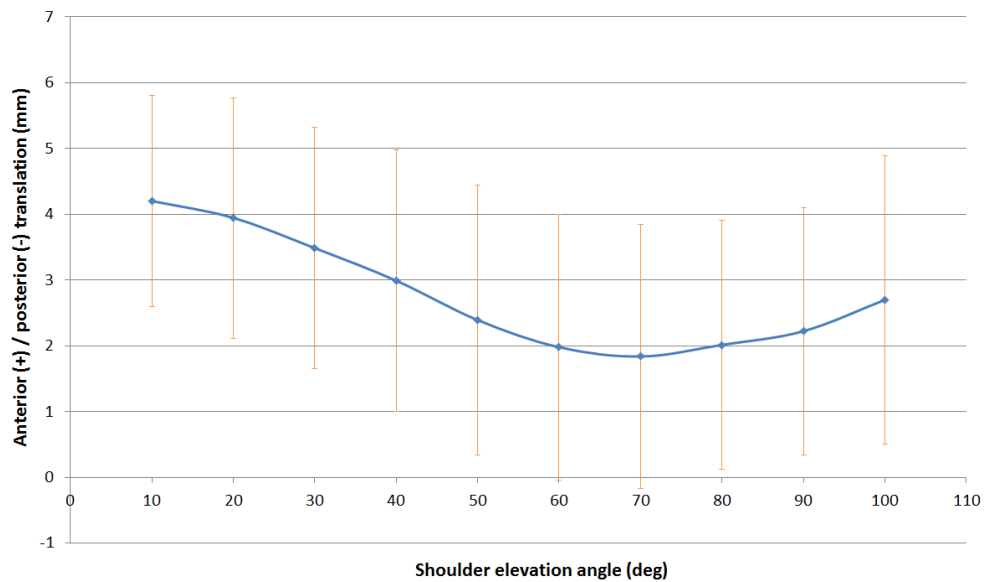
257 During abduction, superior translation of the humeral head in relation to the
258 glenoid was observed until 65°, followed by an inferior translation beyond this
259 amplitude (Figure 7). Consequently, the lateral and anterior subacromial spaces
260 decreased until 65° and then increased progressively. At rest, the humeral head was
261 slightly anteriorly translated. When flexion began, posterior translation was noted

262 until 70° followed by a return to a more anterior translation (Figure 8). There was no
263 posterior subluxation at any degree of flexion.



264

265 **Figure 7:** Superior-inferior translations of the humeral head center relative to the glenoid
266 during abduction. Means and standard deviations for all 10 shoulders.



267

268 **Figure 8:** Anterior-posterior translations of the humeral head center relative to the glenoid
269 during flexion. Means and standard deviations for all 10 shoulders.

270 Also, based on the visual assessment of the 3D simulations, we noticed in six
271 subjects that the arm in abduction was beyond the scapular plane during the cocking

272 stage of serve, resulting in hyperextension.

273

274 **DISCUSSION**

275 Shoulder pain and pathologic lesions are common in overhead athletes. In the
276 present study, 9 of 10 tennis players presented with radiographic signs of structural
277 lesions that could be related to impingement syndrome that occurred with overhead
278 arm movements. However, the precise causes for these lesions remain unclear. It
279 might result from several factors (e.g., repetitive contact, subtle glenohumeral
280 instability, torsional overload with repetitive hypertwisting, scapular orientation and
281 dyskinesia, etc.). The theory of internal impingement in these athletes, which occurs
282 with the arm in the cocked position of 90° abduction, full external rotation and
283 extension,²⁶ holds that repeated contact between the rotator cuff insertion and the
284 posterosuperior glenoid rim lead to articular-sided partial thickness rotator cuff tears
285 and superior labral lesions.^{5,26} If the contact is physiologic, repetitive contact applied
286 at a rate exceeding tissue repair or torsional and shear stresses⁹ may be responsible
287 for rotator cuff or labral damages.

288 This article evaluated dynamically and in-vivo the different aforementioned causes
289 of lesions in tennis players. As shown by the results of this study, anterosuperior and
290 subacromial impingement remain occasional in this particular population. No
291 shoulder instability could be noted during tennis movements. However,
292 posterosuperior impingement was frequent when serving. Thus, as expected, this
293 shot seems to be the most harmful for the tennis player's shoulder. Regarding this
294 type of impingement, repetitive contact could be the cause of posterior and
295 posterosuperior labral lesions, as well as PASTA lesions of the posterosuperior
296 cuff.^{5,27} Indeed, we were not able, as other authors,²⁸ to confirm the role in the

297 impingement development from other culprits like (1) static posterosuperior shifts of
298 glenohumeral contact point leading to torsional overload,⁹ or (2) instability due to
299 gradual repetitive stretching of the anterior capsuloligamentous structures.^{8,26}
300 Nevertheless, this could be explained by the fact that there are many kinds of
301 overhead athletes, and tennis players do not have the same external rotation in
302 abduction and arm speed as do, for example, throwers which have previously been
303 studied. In addition, this could also reflect the efficiency of injury prevention programs
304 that have been established in many tennis clubs (e.g. promotion of compact serve).

305 Concerning subacromial impingement during abduction, superior translation of the
306 humeral head in relation to the glenoid was observed, followed by inferior translation
307 beyond 65°. Such superior and inferior translation confirms previous
308 observations.^{20,29} Consequently, subacromial space decreased until 65° and then
309 increased progressively. Anterior² and lateral³ impingement could hence occur at the
310 beginning of abduction and not at or above 90° like previously believed.³⁰

311 Regarding motion of the glenohumeral joint, the range in internal and external
312 rotation should remain constant between the dominant and the non-dominant arm,
313 with a shift in the external rotation sector of the dominant arm in overhead throwers.⁹
314 We could not confirm the 180° rotation rule in tennis players, as the mean values of
315 the ROM computed in this study were approximately two times smaller than similar
316 measurements found in handball players.³¹ We are, therefore, not convinced that a
317 contracted posterior band, evoking the posterior cable to shorten with resultant
318 GIRD, is a theory that can be extrapolated in tennis players. This theory might be
319 specific to baseball players.

320 Finally, we also evaluated posterior humeral head translation in relation to the
321 glenoid during flexion. An hypothesis of the development of posterior static

322 subluxation described by Walch et al.³² could be posterior subluxation during normal
323 anterior elevation. At rest, the humeral head was slightly anteriorly translated. When
324 forward flexion began, slight posterior translation was noted until 70° followed by a
325 return to a more anterior translation. There was no posterior subluxation at any
326 degree of flexion. Therefore, since no dynamic or physiologic posterior instability was
327 observed, it is probably not responsible (at term) for static instability in these subjects
328 without hyperlaxity.

329 We acknowledge the following limitations in our study: (1) the accuracy of the
330 kinematics computation from motion capture data, which was only validated for low
331 velocity movements. Glenohumeral orientation errors were within 4° for each
332 anatomical plane, which is acceptable for clinical use in the study of shoulder
333 pathology. There is potential for difficulty in the calculation of glenohumeral
334 translation from skin markers due to the high mobility of the shoulder. Although the
335 translations could be significant with our model, we demonstrated in the validation
336 work and in this study that the computed translation patterns and amplitudes were in
337 good agreement with published data. To our knowledge, this non-invasive method is
338 the first attempt to calculate both rotations and translations at the glenohumeral joint
339 based on skin markers. (2) The use of bone-to-bone distances to assess
340 impingement which do not take into account precise measurements of the thickness
341 of the impinged soft tissues. One improvement could be to perform a more advanced
342 simulation accounting for the 3D shapes and movements of cartilages, the labrum
343 and the rotator cuff. (3) The findings may not be generalizable. This was a relatively
344 small sample size of primary males in a single sport and skill level, with a narrow age
345 range. (4) The use of 1.5 T MRI, as stronger magnet strengths would enhance image
346 resolution. Moreover, MRI is not a gold standard to demonstrate bony changes. This

347 study may hence underestimate bony lesions such as Bennett exostosis, and (5) as
348 volunteers were not known for any pathology, a criticism could be to have tested
349 healthy players that would prevent extrapolation of results to complaining patients.
350 However, 9 out of the 10 volunteers reported previous symptoms, so we think that
351 they were a good representation. Despite these limitations, we do believe that they
352 did not call into question the results of this study.

353

354 **CONCLUSION**

355 Tennis players presented frequent radiographic signs of structural lesions that could
356 mainly be related to posterosuperior impingements due to repetitive abnormal motion
357 contacts. This is the first study demonstrating that a dynamic and precise motion
358 analysis of the entire kinematic chain of the shoulder is possible through a non-
359 invasive method of investigation. This premier observation offers novel insights into
360 the analysis of shoulder impingement and instability that could, with future studies, be
361 generalized to other shoulder pathologies and sports. This original method may open
362 new horizons leading to improvement in impingement comprehension.

363

364 ***Practical implications***

- 365 • Anterior and lateral subacromial and posterosuperior impingements are
366 frequent in overhead athletes.
- 367 • Repetitive contact in extreme abduction, extension and external rotation could
368 be the cause of posterior and posterosuperior labral lesions, as well as
369 PASTA lesions of the posterosuperior cuff.
- 370 • Coaches and medical staff should consider promotion of compact serve.

371 • This study has highlighted the benefits of a non-invasive, dynamic and in-vivo
372 evaluation of shoulder pathologies.

373

374 **ACKNOWLEDGMENTS**

375 The authors thank the European Society for Surgery of the Shoulder and the Elbow
376 for their financial support.

REFERENCES

1. Abrams GD, Renstrom PA, Safran MR. Epidemiology of musculoskeletal injury in the tennis player. *Br J Sports Med.* 2012; 46(7):492-498.
2. Neer CS, 2nd. Anterior acromioplasty for the chronic impingement syndrome in the shoulder: a preliminary report. *J Bone Joint Surg Am.* 1972; 54(1):41-50.
3. Nyffeler RW, Werner CM, Sukthankar A, et al. Association of a large lateral extension of the acromion with rotator cuff tears. *J Bone Joint Surg Am.* 2006; 88(4):800-805.
4. Gerber C, Terrier F, Ganz R. The role of the coracoid process in the chronic impingement syndrome. *J Bone Joint Surg Br.* 1985; 67(5):703-708.
5. Walch G, Boileau P, Noel E, et al. Impingement of the deep surface of the supraspinatus tendon on the posterosuperior glenoid rim: An arthroscopic study. *J Shoulder Elbow Surg.* 1992; 1(5):238-245.
6. Gerber C, Sebesta A. Impingement of the deep surface of the subscapularis tendon and the reflection pulley on the anterosuperior glenoid rim: a preliminary report. *J Shoulder Elbow Surg.* 2000; 9(6):483-490.
7. Burkhart SS, Morgan CD, Kibler WB. The disabled throwing shoulder: spectrum of pathology Part III: The SICK scapula, scapular dyskinesis, the kinetic chain, and rehabilitation. *Arthroscopy.* 2003; 19(6):641-661.
8. Jobe CM. Posterior superior glenoid impingement: expanded spectrum. *Arthroscopy.* 1995; 11(5):530-536.
9. Burkhart SS, Morgan CD, Kibler WB. The disabled throwing shoulder: spectrum of pathology Part I: Pathoanatomy and biomechanics. *Arthroscopy.* 2003; 19(4):404-420.
10. Riand N, Levigne C, Renaud E, et al. Results of derotational humeral osteotomy in posterosuperior glenoid impingement. *Am J Sports Med.* 1998; 26(3):453-459.
11. Riand N, Boulahia A, Walch G. Posterosuperior impingement of the shoulder in the athlete: results of arthroscopic debridement in 75 patients. *Rev Chir Orthop Reparatrice Appar Mot.* 2002; 88(1):19-27.
12. Levigne C, Garret J, Grosclaude S, et al. Surgical technique arthroscopic posterior glenoidplasty for posterosuperior glenoid impingement in throwing athletes. *Clin Orthop Relat Res.* 2012; 470(6):1571-1578.

13. Zhu Z, Massimini DF, Wang G, et al. The accuracy and repeatability of an automatic 2D-3D fluoroscopic image-model registration technique for determining shoulder joint kinematics. *Medical Eng & Phys.* 2012; 34(9):1303-1309.
14. Klotz MC, Kost L, Braatz F, et al. Motion capture of the upper extremity during activities of daily living in patients with spastic hemiplegic cerebral palsy. *Gait & Posture.* 2013; 38(1):148-152.
15. Constant CR, Murley AH. A clinical method of functional assessment of the shoulder. *Clin Orthop Relat Res.* 1987(214):160-164.
16. Michener LA, McClure PW, Sennett BJ. American Shoulder and Elbow Surgeons Standardized Shoulder Assessment Form, patient self-report section: reliability, validity, and responsiveness. *J Shoulder Elbow Surg.* 2002; 11(6):587-594.
17. Williams GN, Gangel TJ, Arciero RA, et al. Comparison of the Single Assessment Numeric Evaluation method and two shoulder rating scales. Outcomes measures after shoulder surgery. *Am J Sports Med.* 1999; 27(2):214-221.
18. Roux E, Bouilland S, Godillon-Maquinghen AP, et al. Evaluation of the global optimisation method within the upper limb kinematics analysis. *J Biomech.* 2002; 35(9):1279-1283.
19. Charbonnier C, Chagué S, Kolo F, et al. A patient-specific measurement technique to model the kinematics of the glenohumeral joint. *Orthop & Traumatol: Surg & Res.* 2014; 100(7):715-719.
20. Matsuki K, Matsuki KO, Yamaguchi S, et al. Dynamic in vivo glenohumeral kinematics during scapular plane abduction in healthy shoulders. *J Orthop Sports Phys Ther.* 2012; 42(2):96-104.
21. Wu G, van der Helm FC, Veeger HE, et al. ISB recommendation on definitions of joint coordinate systems of various joints for the reporting of human joint motion - Part II: Shoulder, elbow, wrist and hand. *J Biomech.* 2005; 38(5):981-992.
22. Schneider P, Eberly DH. *Geometric Tools for Computer Graphics (The Morgan Kaufmann Series in Computer Graphics)*, San Francisco, Morgan Kaufmann; 2002.

23. Chopp JN, Dickerson CR. Resolving the contributions of fatigue-induced migration and scapular reorientation on the subacromial space: an orthopaedic geometric simulation analysis. *Hum Mov Sci.* 2012; 31(2):448-460.
24. De Maeseneer M, Van Roy P, Shahabpour M. Normal MR imaging anatomy of the rotator cuff tendons, glenoid fossa, labrum, and ligaments of the shoulder. *Radiol Clin North Am.* 2006; 44(4):479-487, vii.
25. Zumstein V, Kraljevic M, Muller-Gerbl M. Glenohumeral relationships: Subchondral mineralization patterns, thickness of cartilage, and radii of curvature. *J Orthop Res.* 2013; 31(11):1704-1707.
26. Davidson PA, Elattrache NS, Jobe CM, et al. Rotator cuff and posterior-superior glenoid labrum injury associated with increased glenohumeral motion: a new site of impingement. *J Shoulder Elbow Surg.* 1995; 4(5):384-390.
27. Jobe CM. Superior glenoid impingement. Current concepts. *Clin Orthop Relat Res.* 1996; 330:98-107.
28. Halbrecht JL, Tirman P, Atkin D. Internal impingement of the shoulder: comparison of findings between the throwing and nonthrowing shoulders of college baseball players. *Arthroscopy.* 1999; 15(3):253-258.
29. Massimini DF, Boyer PJ, Papannagari R, et al. In-vivo glenohumeral translation and ligament elongation during abduction and abduction with internal and external rotation. *J Orthop Surg Res.* 2012; 7:29.
30. Harrison AK, Flatow EL. Subacromial impingement syndrome. *J Am Acad Orthop Surg.* 2011; 19(11):701-708.
31. Almeida GP, Silveira PF, Rosseto NP, et al. Glenohumeral range of motion in handball players with and without throwing-related shoulder pain. *J Shoulder Elbow Surg.* 2013; 22(5):602-607.
32. Walch G, Asceni C, Boulahia A, et al. Static posterior subluxation of the humeral head: an unrecognized entity responsible for glenohumeral osteoarthritis in the young adult. *J Shoulder Elbow Surg.* 2002; 11(4):309-314.

TABLES

TABLE 1

MRI sequences and their imaging parameters

MRI Sequence	Imaging Parameters
Sagittal T1 weighted fast spin echo without fat saturation	Section thickness 3.5 cm; intersection gap 0.5 cm TR/TE 380/11; FOV 16 x 16 cm
Coronal T2 weighted fast spin echo with fat saturation	Section thickness 4 mm; intersection gap 0.5 cm TR/TE 1920/101,6; FOV 16 x 16cm
Sagittal T2 weighted fast spin echo with fat saturation	Section thickness 3.5 cm; intersection gap 0.5 cm TR/TE 5680/103.5; FOV 16 x 16cm
Coronal T1 weighted fast spin echo with fat saturation	Section thickness 4 mm; intersection gap 0.5 cm TR/TE 320/13; FOV 16 x 16cm
Axial T1 weighted fast spin echo with fat saturation	Section thickness 4 mm; intersection gap 0.5 cm TR/TE 640/26,8; FOV 16 x 16 cm
Axial Cosmic® 3D fast gradient echo with fat saturation	Section thickness 1.8 mm; no intersection gap; TR/TE 6.1/3.0; FOV 28 x 28cm
Axial Cosmic® 3D fast gradient echo without fat saturation	Section thickness 4 mm; no intersection gap; TR/TE 5.7/2.8; FOV 28 x 28cm
Axial Lava® 3D fast gradient echo with fat saturation	Section thickness 5.2 mm; no intersection gap; TR/TE 3.7/1.7; FOV 35 x 35cm

TABLE 2

Shoulder range of motion (deg) determined by motion capture during flexion, empty-can abduction and internal-external rotation with 90° abduction according to the two referentials (n = 30; 10 subjects, 3 trials)

Motion	Humerus motion relative to the thorax		Glenohumeral motion	
	Mean \pm SD	Range	Mean \pm SD	Range
Flexion	144.8 \pm 8.0	125 - 157	98.7 \pm 9.7	83 - 116
Abduction	139.4 \pm 10.9	119 - 161	88.8 \pm 11.8	65 - 108
Internal rotation (IR)	44.0 \pm 9.8	30 - 70	22.3 \pm 11.1	11 - 45
External rotation (ER)	52.6 \pm 10.8	36 - 77	58.6 \pm 10.3	43 - 79
Total IR-ER	96.6 \pm 17.5	74 - 147	80.8 \pm 14.9	60 - 107

TABLE 3

Frequency of impingement and minimum humero-acromial, humero-coracoid and humero-glenoid distances (mm) at critical tennis positions (n = 30; 10 subjects, 3 trials)

Distances	Flat serve	Kick serve	Forehand	Backhand
	Frequency Mean \pm SD	Frequency Mean \pm SD	Frequency Mean \pm SD	Frequency Mean \pm SD
Lateral humero-acromial	29% 7.5 \pm 3.2	42% 6.8 \pm 3.7	-	-
Anterior humero-acromial	29% 7.4 \pm 2.9	29% 7.0 \pm 3.1	-	-
Humero-coracoid	-	-	0% 15.9 \pm 1.6	0% 15.0 \pm 2.7
Anterosuperior humero-glenoid	-	-	29% 5.5 \pm 1.2	0% 6.9 \pm 1.3
Posterosuperior humero-glenoid	76% 3.6 \pm 1.4	75% 3.3 \pm 1.8	-	-

TABLE 4

Pourcentage of subluxation of the glenohumeral joint during tennis serves (n = 30; 10 subjects, 3 trials)

Shot, position	Anterior-posterior subluxation*		Superior-inferior subluxation†	
	Mean ± SD	Range	Mean ± SD	Range
Flat serve, late cocking stage	34% ± 9%	14% - 47%	12% ± 6%	-1% - 21%
Kick serve, late cocking stage	34% ± 6%	22% - 44%	13% ± 9%	0% - 32%
Flat serve, deceleration stage	34% ± 14%	8% - 57%	18% ± 7%	8% - 34%
Kick serve, deceleration stage	37% ± 9%	20% - 56%	19% ± 7%	5% - 32%
Flat serve, finish stage	46% ± 15%	18% - 68%	3% ± 5%	-5% - 14%
Kick serve, finish stage	42% ± 13%	17% - 67%	10% ± 8%	0% - 30%

* A positive value means that the subluxation is anterior, otherwise it is posterior.

† A positive value means that the subluxation is superior, otherwise it is inferior.